L-32 THE EFFECT OF SEISMIC ANISOTROPY ON MULTICOMPONENT IMAGING AND AVO

J. O. HANSEN[1] and A. BAKULIN[2]
[1] Schlumberger Stavanger Research, P.O.Box 8013, 4068 Stavanger, Norway
[2] Schlumberger Cambridge Research

Summary

This paper shows how seismic anisotropy affects the imaging and AVO of multicomponent seabed data acquired over the Siri reservoir in the North Sea. Model-based processing is used to analyze the data and compare results from isotropic and anisotropic velocity models. A layered vertically transversely isotropic (VTI) model was used in this study, constructed by Grechka et al. (2001). Neglecting the overburden anisotropy causes 0–550 m smearing of the reflection points of converted *PS*-waves at the target level and results in false *PS* AVO. Such smearing greatly degrades the fault imaging above the Siri reservoir. When compared to an isotropic model, overburden anisotropy can also change offset-to-angle mapping by up to 8 degrees for *PS* data and 2.5 degrees for *PP*.

Introduction

Combining *PP* and *PS* data has the potential of constraining the subsurface shear-velocity field and reducing the uncertainty in lithology or fluid inversion. The higher sensitivity of *PS* AVO to contrasts in shear velocity (V_S) and density (ρ) makes it a promising tool, especially when *PP* AVO fails to distinguish between hydrocarbon-saturated rocks and other lithologies. Since the *PS* reflection coefficient is zero at normal incidence, both the contrasts in V_S and ρ are embedded into the gradient, and angles up to 40 degrees have to be included to obtain reliable estimates of rock properties (Jin et al., 2000).

Isotropic processing of converted-wave data can potentially introduce significant errors in the offset-to-angle mapping and can thus severely distort the results of *PS* AVO inversion. Furthermore, the assumption of an isotropic overburden model may result in large smearing of the *PS* reflection point, which both limits the lateral resolution and affects the AVO (Thomsen, 1999).

We quantify the effects of anisotropy on imaging (reflection point smearing) and offset-to-angle mapping using a 2-D 4C data set acquired over the Lower Tertiary Siri reservoir in the North Sea.

Model-based multicomponent processing

The Siri survey consists of 3-D surface towed streamer data and three 4-C seabed lines. A description of the acquisition, isotropic processing and interpretation can be found in Signer et al. (2000). Analysis of one of the 4C lines was performed using a model-based processing approach, which includes:

1) Pre-stack picking of *PP* and *PS* reflection times on common-receiver gathers for all layers in the model.
2) Building of an anisotropic macro-velocity model consistent with both *PP* and *PS* data (Grechka et al., 2001).
3) For each model layer, both the anisotropic moveout and the common-conversion point (CCP) trajectory in the receiver-offset plane are calculated from ray-tracing modeling and used in the subsequent CCP stacking.
4) The anisotropic model is further used to map between offsets and angles in order to build generalized *PP* and *PS* AVO sections (Sønneland et al., 1996).

Pre-stack picking

Pre-stack horizon-consistent picking was achieved in several steps. First, an initial *P*-wave velocity model was built from 3-D surface seismic data. Then correlation of a brute *PS* and *PP* stacks provided an initial estimate of *S*-wave velocity field. Using short-offset *PS* data, an isotropic model-based CCP stack was produced by extraction of both the sorting and the moveout trajectories from ray tracing in the isotropic depth model. To improve the consistency, this was followed by a second pass of event correlation between *PP* and *PS* stacked data. Finally, pre-stack horizon-consistent traveltime curves were picked on common-receiver gathers of *PP* and *PS* data. Picking was guided both by ray tracing and by zero-offset traveltimes of correlated events from stacked sections.

Building the anisotropic velocity model

Iversen et al. (2000) showed that obtained pre-stack *PP* and *PS* traveltime picks can be used in a map migration approach in order to estimate interval anisotropic parameters. However, this method relied on the assumption that initial depths of the horizons (taken from isotropic processing) did not change. In this study, we have chosen to use a different approach addressing the model building in two steps. First, pure *SS*-wave reflection traveltimes are extracted from *PP* and *PS* pre-stack traveltimes using the methodology of Grechka and Tsvankin (2001a). Interval anisotropic parameters are then estimated by means of joint stacking-velocity tomography of *PP* and *SS* data (Grechka and Tsvankin, 2001b), assuming a model of homogeneous VTI layers with arbitrary dipping interfaces.

Inversion performed for part of the line ($7\ km < X_{CMP} < 10\ km$, see Figure 1) shows that the structure above the Siri reservoir is close to horizontally layered, and a unique VTI model cannot be found, even though long-spread (i.e. more than twice the reflector depths) *PP* and *PS* data are available (Grechka et al., 2001). A family of equivalent anisotropic models, that fit the observed traveltimes equally well, was constructed. Each model satisfies the approximate relationship $\varepsilon = 0.06+1.25\delta$ between the Thomsen anisotropy coefficients ε and δ. This implies that the isotropic medium ($\varepsilon = \delta = 0$) cannot adequately describe the data. The layered model with $\delta = 0$ [Figure 3a in the companion paper by Grechka et al. (2001)] was selected as input for the anisotropic model-based CCP imaging and AVO calculations. The same model but with ε and δ set to zero ($\varepsilon = \delta = 0$) is further referred to as the "isotropic velocity model" and used for comparison purposes. In the isotropic model, *P*- and *S*-velocities are angle-independent and equal to vertical velocities in the correct VTI model.

Isotropy vs. anisotropy

Comparison of model-based isotropic (Figure 1a,c) and anisotropic (Figure 1b,d) *PS* CCP stacks obtained using two different velocity models reveals two main advantages of anisotropic imaging. First, temporal resolution is greatly improved mainly due to use of correct normal moveout (NMO) velocities. Secondly, significant enhancement in fault imaging is obtained by using correct CCP sorting trajectories, which account for overburden anisotropy. Figures 1e and 1f confirm that NMO velocities have the largest effect on the apparent temporal resolution; however they do not greatly improve lateral resolution. Figures 1d and 1f prove that significantly better definition of the center faults occurs only when the CCP trajectories are taken from the correct VTI model and therefore anisotropy is completely honored.

Poor imaging of the faults by the isotropic model may be explained by smearing of the *PS* reflection point occurring due to anisotropy and layering (Thomsen, 1999). For short spreads, asymptotic conversion points X^{ISO} and X^{VTI} [horizontal distances between the source and image (conversion) point] can be approximated as:

$$X^{ISO}=X/(1+g_0),\quad X^{VTI}=X/(1+g_{nmo}), \tag{1}$$

where X is the source-receiver offset (Thomsen, 1999). Ratios of vertical velocities $g_0=V_{S0}/V_{P0}$ (≈ 0.35) and normal moveout velocities $g_{nmo}=V_{S,nmo}/V_{P,nmo}$ (≈ 0.5) for the target horizon shown on Figure 2, provide the short-spread ($X < 2000\ m$) approximation $X^{ISO} - X^{VTI} = 0.16\,X$. This is consistent with the initial part of the model-based curve on Figure 3a. As expected, the true image point in the VTI model is closer to the source than in the incorrect isotropic model (Thomsen, 1999).

Clearly such a lateral shift limits the spatial resolution and does not only bias the observed *PS* AVO, but results in false AVO as the isotropic sorted gather includes reflections from a range of sub-surface points. Error in the offset-to-angle transformation for an isotropic model versus the anisotropic model is shown on Figure 3b. For *PS* reflections, the discrepancy is up to 8 degrees for 3000-meter offset (depth ~2000 m), whereas for *PP* it is up to 2.5 degrees.

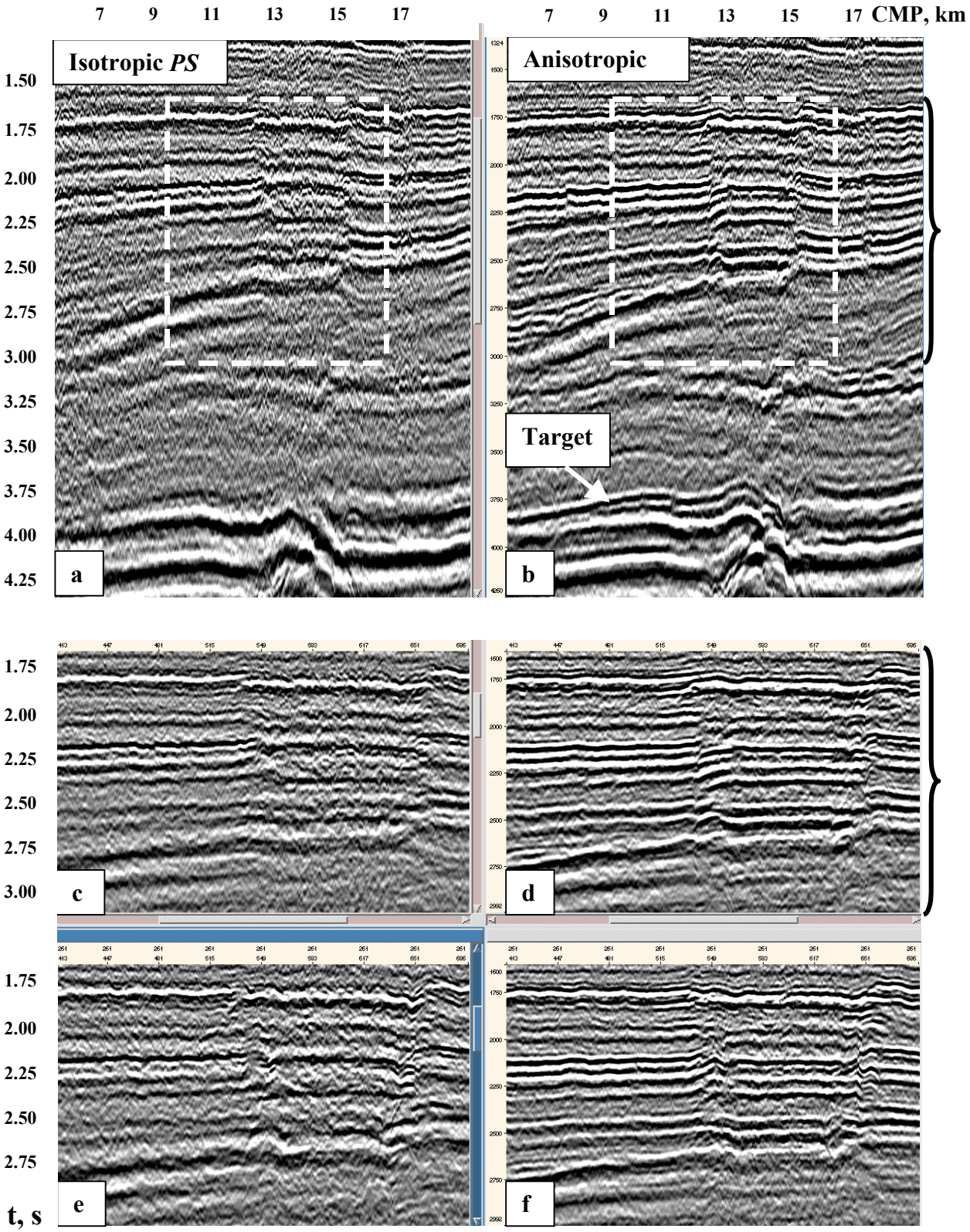

Figure 1: Model-based common-conversion point stacks of *PS* data (all offsets):
(a) isotropic vs. (b) anisotropic (VTI).
PS imaging with separated moveout and CCP sorting:
(c) isotropic moveout and isotropic CCP sorting, (d) anisotropic moveout and anisotropic CCP sorting,
(e) isotropic moveout and anisotropic CCP sorting, (f) anisotropic moveout and isotropic CCP sorting.

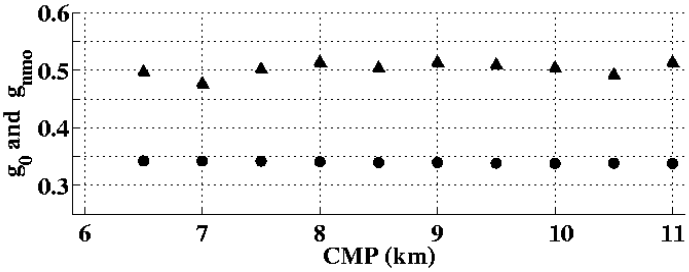

Figure 2: Ratio of vertical $g_0=V_{S0}/V_{P0}$ (circles) and NMO $g_{nmo}=V_{S,nmo}/V_{P,nmo}$ (triangles) velocities for the target horizon.

Conclusions

Seismic anisotropy cannot be neglected when imaging *PS* multicomponent data. This is especially important if *PS* AVO is used for reservoir characterization purposes, since overburden anisotropy significantly changes both the offset-to-angle mapping and the lateral positioning of the conversion point. The assumption of an isotropic overburden may severely reduce both the spatial and temporal resolution so that the resulting image cannot be used for detailed interpretation and analysis.

References

Grechka, V., Tsvankin, I., Bakulin, A., and Hansen, J.O., 2001, Joint inversion of *PP* and *PS* reflection data for VTI medium: a North Sea case study: 63rd EAGE Conference, Amsterdam, this volume.

Grechka, V., and Tsvankin, I., 2001a, *PP+PS=SS* : 63rd EAGE Conference, Amsterdam, this volume.

Grechka, V., and Tsvankin, I., 2001b, Parameter estimation for VTI media using *PP* and *PS* reflection data: 63rd EAGE Conference, Amsterdam, this volume.

Iversen, E., Gjøystdal, H., and Hansen, J.O., 2000, Prestack map migration as an engine for parameter estimation in TI media: 70th Ann. Internat. Mtg., Soc. Expl. Geophys., Expanded Abstracts, 1004-1007.

Jin, S., Cambois, G., and Vuillermoz, C., 2000, Shear-wave velocity and density estimation from *PS*-wave AVO analysis: Application to an OBS dataset from the North Sea: Geophysics, **65**, 1446-1454.

Signer, C., Hansen, J.O., Hutton, G., Nickel, M., Reymond, B., Schlaf, J., Sønneland, L., Tjøstheim, B., and Veire, H.H., 2000, Reservoir characterization using 4C seismic and calibrated 3D AVO: in Improving the Exploration Process by Learning from the Past, Eds: Ofstad, K., Kittilsen, J.E., and Alexander-Marrack, P., Elsevier Science.

Sønneland, L., Thornsteinsen, H.H., and Hansen, J.O., 1996, Model-based AVO-inversion: 58nd EAGE Conference and Technical Exhibition, Extended Abstracts, Amsterdam, V.1, M047.

Thomsen, L., 1999, Converted-wave reflection seismology over inhomogeneous, anisotropic media: Geophysics, **64**, 678-690.

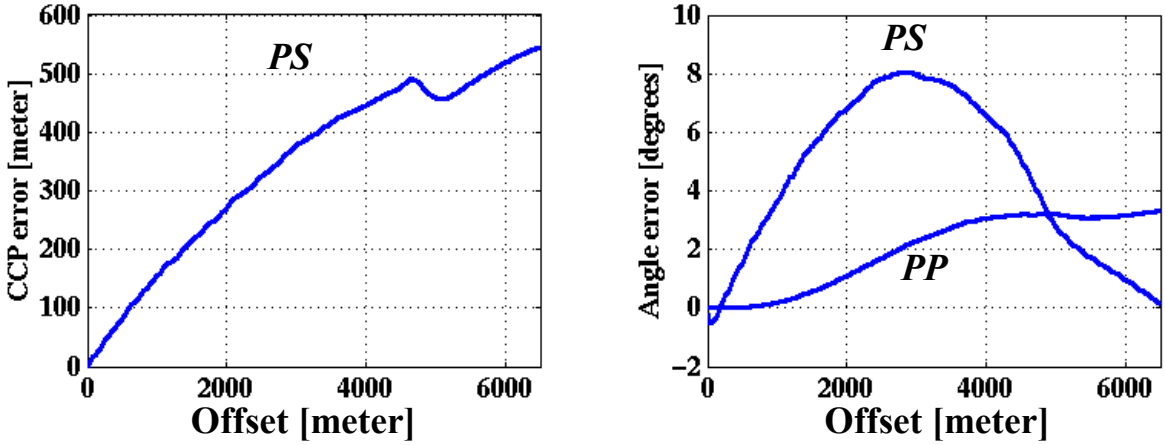

Figure 3: (a) *PS* CCP reflection point error ($X_{ISO} - X_{VTI}$) and (b) *P*-leg incident angle error ($\theta_{ISO} - \theta_{VTI}$) as a functions of source-receiver offset for the target horizon (Figure 1) in isotropic model.